Odgen, S., Haggerty, D., Stoner, C. M., Kolodrubetz, D., & Schleif, R. (1980) *Proc. Natl. Acad. Sci. U.S.A. 77*, 3346-3350.
Oida, T. (1977) Master Thesis, The University of Tokyo.
Pastan, I., & Perlman, R. L. (1970) *Science (Washington, D.C.) 169*, 339-344.
Plochocka, D., Rabczenky, A. R., & Davies, D. B. (1977) *Biochim. Biophys. Acta 476*, 1-15.
Poulson, F. M., Hosch, J. C., & Dobson, C. M. (1980) *Biochemistry 19*, 2597-2607.
Rao, S. T., & Sundaralingam, M. (1970) *J. Am. Chem. Soc. 92*, 4963-4970.
Redfield, A. G., & Gupta, R. K. (1971) *Cold Spring Harbor Symp. Quant. Biol. 36*, 405-419.
Riggs, A. D., Reiness, G., & Zubay, G. (1971) *Proc. Natl. Acad. Sci. U.S.A. 68*, 1222-1225.
Takahashi, M., Blazy, B., & Baudras, A. (1980) *Biochemistry 19*, 5124-5130.
Taniguchi, T., O'Neill, M., & de Crombrugghe, B. (1979) *Proc. Natl. Acad. Sci. U.S.A. 76*, 5090-5094.
Wagner, G., Kumar, A., & Wüthrich, K. (1981) *Eur. J. Biochem. 114*, 375-384.
Wu, C. W., & Wu, F. Y. H. (1974) *Biochemistry 13*, 2573-2578.
Wyeth, P., Gronenborn, A., Birdsall, B., Roberts, G. C. K., Feeney, J., & Burgen, A. S. V. (1980) *Biochemistry 19*, 2608-2615.
Yathindra, N., & Sundaralingam, M. (1974) *Biochem. Biophys. Res. Commun. 56*, 119-126.
Zubay, G., Schwartz, D., & Beckwith, J. (1970) *Proc. Natl. Acad. Sci. U.S.A. 66*, 104-110.

Proton Nuclear Magnetic Resonance Study of the Histidine Residues of the *Escherichia coli* Adenosine Cyclic 3′,5′-Phosphate Receptor Protein. pH Titration Behavior, Deuterium Exchange, and Partial Assignments†

G. M. Clore* and A. M. Gronenborn*

ABSTRACT: The properties of the histidine residues of the cyclic AMP receptor protein (CRP) of *Escherichia coli* and its N-terminal core (αCRP) have been investigated by ^{1}H NMR. Comparison of the spectra of CRP and αCRP shows that of the five histidine residues per subunit present in CRP, three, histidines A, C, and D, lie in the N-terminal domain, and two, histidines B and E, lie in the smaller carboxy-terminal domain. The C(2) protons of histidines A, B, C, and D undergo rapid deuterium exchange at 37 °C with a $t_{1/2}$ of about 2 days, in contrast to that of histidine E, which remains unexchanged after 50 days. With the exception of histidine E, complete pH titration curves were obtained for the histidine residues. The pH titration curves for the imidazole proton resonances of the three histidine residues, A, C, and D, present in the N-terminal core are identical in CRP and αCRP. The pH titration curves of the imidazole proton resonances of histidines A and B exhibit classical Henderson-Hasselbach behavior, titrating with a single pK. In contrast, the pH titration curves for the imidazole proton resonances of histidines C and D deviate markedly from Henderson-Hasselbach behavior and can be described quantitatively by a model in which their imidazole rings mutually interact. Partial assignments of the histidine residues are discussed on the basis of the data presented in this paper and data in the literature on the X-ray crystal structure of CRP [McKay, D. B., & Steitz, T. A. (1981) *Nature (London) 290*, 745-749] and on the nucleotide sequence of its structural gene [Aiba, H., Fujimoto, S., & Ozaki, N. (1982) *Nucleic Acids Res. 10*, 1345-1362; Cossart, P., & Gicquel-Sanzey, B. (1982) *Nucleic Acids Res. 10*, 1363-1378].

In the preceding paper (Gronenborn & Clore, 1982), we presented a ^{1}H nuclear magnetic resonance (NMR)[1] study on the binding of cyclic nucleotides to the cyclic AMP receptor protein (CRP) of *Escherichia coli*. CRP is a dimer of apparently identical subunits, each of molecular weight 22 500 (Anderson et al., 1971; Riggs et al., 1971). X-ray crysallographic studies (McKay & Steitz, 1981) have shown that each subunit is composed of two domains, a larger N-terminal domain which contains the cyclic nucleotide binding site and a smaller carboxy-terminal domain which was proposed to contain the DNA binding site. Subtilisin digestion of the cAMP·CRP complex separates these two domains and results in the formation of a stable N-terminal core, αCRP, in which each subunit has a molecular weight of 12 500 (Krakow & Pastan, 1973; Eileen et al., 1978). αCRP retains the ability to bind cAMP (Krakow & Pastan, 1973) and more recently has been shown to bind DNA nonspecifically, stabilizing its double-helical structure (Takahashi et al., 1981). In the present paper, we present a detailed study by ^{1}H NMR of the histidine residues of CRP and αCRP. The possible assignments of the histidine residues are discussed in relation to the amino acid sequence of CRP deduced from the nucleoside sequence of its structural gene (Aiba et al., 1982; Cossart & Gicquel-Sanzey, 1982) and X-ray crystallographic data (McKay & Steitz, 1981).

Experimental Procedures

Materials. CRP was purified from *E. coli* KLF 41 by the method of Takahashi et al. (1980). αCRP was prepared by

† From the Division of Molecular Pharmacology, National Institute for Medical Research, Mill Hill, London NW7 1AA, United Kingdom. *Received January 8, 1982.*

[1] Abbreviations: CRP, cyclic AMP receptor protein; αCRP, N-terminal core of CRP; NMR, nuclear magnetic resonance; NOE, nuclear Overhauser effect; SD_{ln}, standard deviation of the natural logarithm of an optimized parameter; $NaDodSO_4$, sodium dodecyl sulfate; EDTA, ethylenediaminetetraacetic acid.

0006-2960/82/0421-4048$01.25/0

subtilisin digestion of the cAMP·CRP complex by a modification (B. Blazy, M. Takahashi, and A. Baudras, unpublished results) of the procedure described by Eilen et al. (1978). Both CRP and αCRP were greater than 99% pure as judged by $NaDodSO_4$–polyacrylamide gel electrophoresis (with apparent molecular weights on the gels of 22 500 ± 500 and 12 500 ± 500 for the constituent polypeptide chains of CRP and αCRP, respectively). All chemicals were of the highest purity commercially available.

Sample Preparation. Samples for ^{1}H NMR were prepared by dialyzing extensively 0.56 mM CRP or αCRP against D_2O containing 50 mM potassium phosphate, pH* 6.5 (meter reading uncorrected for the isotope effect on the glass electrode), 500 mM KCl, and 1 mM EDTA.

The pH of the samples was adjusted by the addition of microliter volumes of 0.1–1.0 M KOD or DCl [>99% atom % D; CIBA (ARL) Ltd.] and measured by using a combination glass/reference electrode and a Radiometer Model 26 pH meter. The pH* was checked after each recording of a spectrum, and the spectrum was accepted only if this was within 0.04 pH unit of the reading before the spectrum was acquired.

NMR Spectroscopy. ^{1}H NMR spectra were recorded at 270 MHz on a Bruker WH 270 spectrometer as described previously (Gronenborn & Clore, 1982). Chemical shifts are expressed relative to internal 1 mM dioxane (3.71 ppm downfield from 4,4-dimethyl-4-silapentane-1-sulfonate). All spectra were recorded at 20 °C. Intraresidue NOE's between the histidine C(4) and C(2) proton resonances were measured by using the pulse sequence t_1–t_2–$\pi/2$–AT–t_3 where the selective irradiation at a chosen frequency is applied during the time interval t_1 (0.2 s), t_2 is a short delay (2 ms) to allow for electronic recovery after removal of the selective irradiation, AT is the acquisition time (0.974 s), and t_3 is a delay (1 s) to allow for recovery of magnetization. A total of 5000 scans were averaged for each NOE experiment.

Data Analysis. The histidine pH titration data were analyzed by fitting the experimental data to appropriate mathematical models by using Powell's (1972) method of nonlinear optimization as described previously (Clore & Chance, 1978). In all cases, the data for the C(2) proton resonance of a given histidine residue were fitted simultaneously with the data for the corresponding C(4) proton resonance with the exception of a single histidine residue, histidine E, for which the C(4) proton resonance could not be identified. This was carried out to ensure that a given set of C(2) and C(4) proton resonances belonged to the same histidine residue, as a difference in pK of $\lesssim$0.1 unit between the pH titration curves for a C(2) and C(4) proton would be picked up in the form of systematic errors between the calculated and observed curves.

Results

Histidine Residues in CRP and αCRP. Figure 1 shows the aromatic region of the ^{1}H NMR spectrum of CRP and αCRP. It can be clearly seen that of the five sets of histidine resonances seen in the spectrum of CRP, those of two of the histidine residues, B and E, are absent in the spectrum of αCRP. We therefore deduce that histidine residues B and E reside in the small carboxy-terminal domain of CRP. The chemical shifts of the imidazole proton resonances of the other three histidine residues, A, C, and D, are identical in CRP and αCRP, indicating that their environment in αCRP is unperturbed with respect to that in CRP. It is also interesting to note that the line widths of both the C(2) and C(4) proton resonances of histidines A, C, and D are identical in CRP αCRP, despite the fact that the molecular weight of αCRP

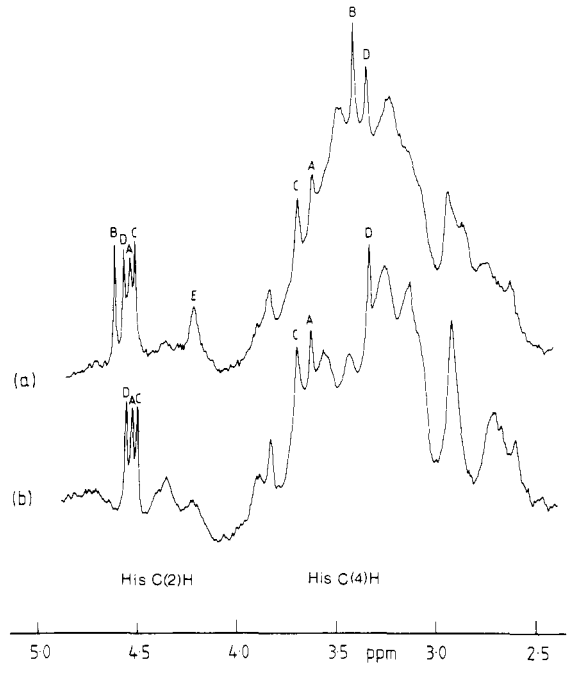

FIGURE 1: ^{1}H NMR spectrum at 270 MHz of the aromatic region of (a) CRP and (b) αCRP. Experimental conditions: 0.28 mM CRP or αCRP in D_2O containing 50 mM potassium phosphate, pH* 6.5, 500 mM KCl, 1 mM EDTA, and 1 mM dioxane. The chemical shifts are expressed relative to internal dioxane (3.71 ppm from 4,4-dimethyl-4-silapentane-1-sulfonate). The spectra were recorded at 20 °C.

is 20 000 less than that of CRP. This strongly suggests that the mobility of the region in which these histidine residues lie is unchanged in both CRP and αCRP.

The C(4) and C(2) proton resonances of histidines A and D could be connected by the measurement of intraresidue NOE's. In the case of CRP, irradiation for 0.2 s of the C(4) proton resonance of histidine A resulted in a selective decrease of −6% in the intensity of the corresponding C(2) proton resonance; similarly, irradiation of the C(4) proton resonance of histidine D resulted in a −10% decrease in the intensity of its corresponding C(2) proton resonance. We could not, however, detect NOE's from the C(4) protons of histidines B and C to their corresponding C(2) protons. Demonstration of selective NOE's from the C(2) to the C(4) protons was not possible, owing to the fact that the C(2) proton resonances of histidines A–D are too close together in the spectrum.

Deuterium Exchange of the Histidine C(2) Proton Resonances in CRP. The histidine C(2) proton resonances of CRP are shown in Figure 2 as a function of the length of time of incubation in D_2O at 37 °C. The rate of exchange of the C(2) proton resonances of the four histidine residues, A–D, is fast with a $t_{1/2}$ of about 2 days. This is consistent with their residing in a mobile portion of the protein. The C(2) proton of histidine E, however, remains completely unexchanged after 50 days (Figure 2). Thus, histidine E must be buried inside the protein so that its C(2) proton is inaccessible to the solvent and, in addition, must be immobilized to a certain extent to account for its large line width (~15 Hz).

pH Dependence of the Histidine Resonances of CRP and αCRP. Complete titration curves for all the histidine resonances with the exception of the C(2) proton resonance of histidine E were obtained (Figures 3 and 4). The titration curves for the three histidine residues, A, C, and D, present in the N-terminal core were identical in CRP and αCRP. It should be noted that the broad resonances in the imidazole proton region around 4.35, 4.22, and 3.84 ppm present in both

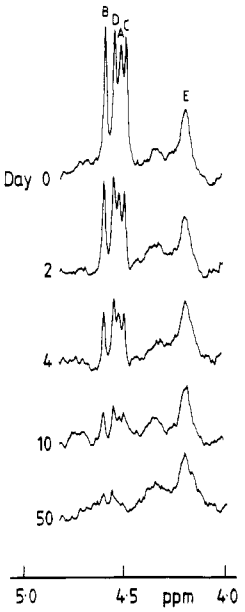

FIGURE 2: Histidine C(2) proton resonances of CRP as a function of the length of time of incubation in D_2O at 37 °C and pH* 6.5. The experimental conditions are given in the legend to Figure 1. The spectra were recorded at 20 °C.

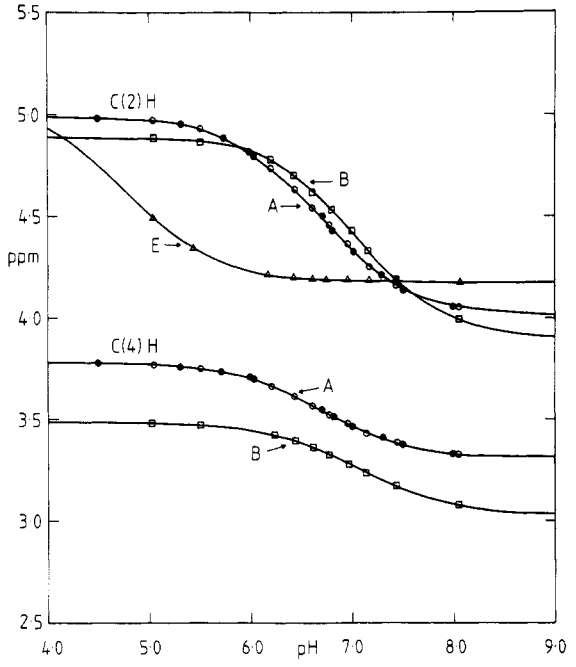

FIGURE 3: pH dependence of the chemical shift of the imidazole proton resonances of histidines A, B, and E in CRP and of histidine A in αCRP. The experimental data are shown as (○ and ●) imidazole proton resonances of histidine A in CRP and αCRP, respectively, (□) imidazole proton resonances of histidine B in CRP, (△) C(2) proton resonance of histidine E in CRP [the corresponding C(4) proton resonance was not observed]. The continuous lines (—) are the best-fit theoretical curves obtained by fitting the experimental data to the Henderson–Hasselbach equation. In the case of histidines A and B, the pH titration data for the C(2) and C(4) proton resonances were fitted simultaneously. The values of the optimized parameters (pKs and chemical shift parameters) are given in Table I. The experimental conditions are given in the legend to Figure 1.

CRP and αCRP did not exhibit a pH-dependent chemical shift over the pH* range 4.5–8.0. [Note that the broad resonance around 4.22 ppm in αCRP lies underneath the C(2) proton resonance of histidine E in CRP at pH* 6.5; see Figure 1.] Moreover, these resonances did not undergo deuterium exchange over a period of 50 days at 37 °C. We suggest that

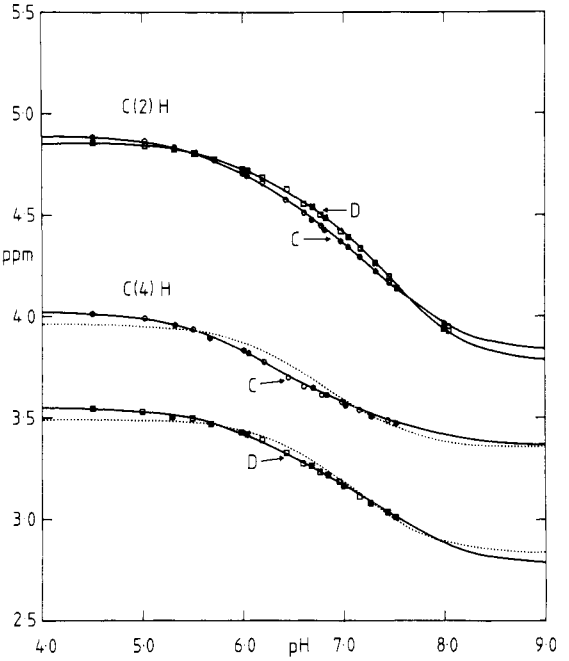

FIGURE 4: pH dependence of the chemical shift of the imidazole proton resonances of histidines C and D in CRP and αCRP. The experimental data are shown as (○ and ●) imidazole proton resonances of histidine C in CRP and αCRP, respectively, and (□ and ■) imidazole proton resonances of histidine D in CRP and αCRP, respectively. The continuous lines (—) are the best-fit theoretical curves obtained by fitting all the experimental data simultaneously to models for mutual interaction between two titrating imidazole groups given by eq 4 and 5. The best-fit curves for models 1 ($K_{C0} = K_{D0}$, $\alpha \neq 1$) and 2 ($K_{C0} \neq K_{D0}$, $\alpha = 1$) are indistinguishable. The values of the optimized parameters (microscopic association constants, chemical shift parameters, and dimensionless constants) are given in Table II. The dashed lines (---) represent the best-fit curves obtained by fitting the data for each histidine residue to the Henderson–Hasselbach equation [these are only shown for the C(4) proton resonance for clarity]; the optimized values of the pKs obtained in this manner are 6.77 and 7.03 for histidines C and D, respectively. The experimental conditions are given in the legend to Figure 1.

the broad resonances at 4.35 and 4.22 ppm most probably arise from very slowly exchangeable NH groups of the protein backbone.

The pH dependence of the chemical shift of the C(2) proton resonance of histidine E over the pH range studied for CRP (pH 5–8) was too small to calculate an accurate value for the pK other than determining an upper limit of ~5. The pH dependence of the imidazole proton resonances of histidines A and B shows classical Henderson–Hasselbach behavior, titrating with a single pK of 6.68 and 7.06, respectively. The pKs and chemical shifts in the protonated and unprotonated states for the imidazole proton resonances of histidines A, B, and E are collected in Table I.

In the case of the titration curves for the imidazole protons of histidines C and D, clear deviations from Henderson–Hasselbach behavior are seen (Figure 4). The data were analyzed in terms of a model for interacting sites (Edsall et al., 1958; Schrager et al., 1972):

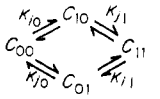

(1)

where C_{00} and C_{11} are the concentrations with both sites unoccupied and occupied, respectively, C_{10} is the concentration with the first site occupied and the second site unoccupied, and C_{01} is the concentration with the first site unoccupied and the second site occupied. If a proton is assumed to be the sole

Table I: pK Values, Chemical Shifts, and Protonation Shifts of Histidine A in CRP and αCRP and of Histidines B and E in CRP[a]

histidine residue	pK[b]	chemical shift parameters[c] (ppm from dioxane) C(2) proton resonance δ_0	δ_1	$\Delta\delta$	C(4) proton resonance δ_0	δ_1	$\Delta\delta$
A	6.68	4.01	4.99	0.98	3.31	3.78	0.47
B	7.06	3.90	4.89	0.99	3.03	3.48	0.45
E	4.82	4.18	5.05	0.87			

[a] Values were obtained by fitting the experimental pH titration data for each histidine residue in Figure 3 to a single Henderson-Hasselbach expression. δ_0 is the unprotonated state, δ_1 is the protonated state, and $\Delta\delta$ is the protonation shift. [b] The standard deviation of the pK values is ±0.01 unit with the exception of that for the pK of histidine E, which is ±0.2 unit. [c] The standard deviation of the chemical shift parameters is ±0.01 ppm with the exception of that for the chemical shift of the C(2) proton resonance of histidine E in the protonated state, δ_1, which is ±0.05 ppm.

occupant of each site, the microscopic association constants are defined

$$K_{i0} = C_{10}/(C_{00}[H^+]) \qquad K_{j0} = C_{01}/(C_{00}[H^+])$$
$$K_{i1} = C_{11}/(C_{01}[H^+]) \qquad K_{j1} = C_{11}/(C_{10}[H^+]) \quad (2)$$
$$K_{i0}K_{j1} = K_{i1}K_{j0}$$

where the first subscript refers to the site in question (i or j) and the second to the state of the other site (0 or 1). The cooperativity parameter, α, describing eq 1 is defined

$$\alpha = K_{i1}/K_{i0} = K_{j1}/K_{j0} \quad (3)$$

The derivation of the equations describing the pH dependence of the chemical shift in such a system has been described in detail by Schrager et al. (1972), and only the final equations will be given here. The chemical shifts (δ) of the resonance(s) of sites i and j are given by

$$\delta_i = \frac{\delta_{i00} + (K_{i0}\delta_{i10} + K_{j0}\delta_{i01})[H^+] + K_{i1}K_{j0}\delta_{i11}[H^+]^2}{1 + (K_{i0} + K_{j0})[H^+] + K_{i1}K_{j0}[H^+]^2} \quad (4)$$

$$\delta_j = \frac{\delta_{j00} + (K_{j0}\delta_{j10} + K_{i0}\delta_{j01})[H^+] + K_{i1}K_{j0}\delta_{j11}[H^+]^2}{1 + (K_{i0} + K_{j0})[H^+] + K_{i1}K_{j0}[H^+]^2} \quad (5)$$

where δ_{xlm} is the chemical shift parameter, the first subscript referring to the site of the monitored resonance, the second to the state of site i, and the third to the state of site j.

It will be noted that δ_{x01} and δ_{x10} *cannot* be determined independently and *must* be combined into a *single* intermediate chemical shift parameter γ_x. This is achieved by setting the terms $K_{x0}\delta_{x10} + K_{y0}\delta_{x01}$ in eq 4 and 5 equal to $\gamma_x(K_{x0} + K_{y0})$ where γ_x is defined

$$\gamma_x = (K_{x0}\delta_{x10} + K_{y0}\delta_{x01})/(K_{x0} + K_{y0}) = \delta_{x00} + \rho_x(\delta_{x11} - \delta_{x00}) \quad (6)$$

and ρ_x is a dimensionless constant. When this is done, *no* assumptions regarding intermediate chemical shifts are required to fit the data.

We analyzed the pH titration data for the C(2) and C(4) proton resonances of histidines C and D *simultaneously* on the basis of mutual interaction between the two titrating imidazole groups. In the initial optimizations, we varied the microscopic association constants K_{C0} and K_{D0}, the cooperativity parameter α, the chemical shift parameters δ_{x00} and δ_{x11} of the fully unprotonated and fully protonated species, respectively, for all the proton resonances, and the dimensionless constant ρ_x for all the proton resonances. The chemical shift parameters and dimensionless constants were all well determined; K_{C0}, K_{D0}, and α, however, were very poorly determined and, in addition, highly correlated (see Table II). In the subsequent optimizations, we therefore considered two alternative models:

Table II: Overall Standard Deviations of the Fits, Mean Absolute Correlation Indices, and Values of the Optimized Parameters for Histidines C and D[a]

	$K_{C0} \neq K_{D0}$; $\alpha \neq 1$	model 1: $K_{C0} = K_{D0}$; $\alpha \neq 1$	model 2: $K_{C0} \neq K_{D0}$; $\alpha = 1$
K_{C0} (M^{-1})	7.85×10^6 (>5)[b]	1.46×10^7 (0.12)	1.64×10^6 (0.13)
K_{D0} (M^{-1})	2.10×10^7 (>5)[b]	1.46×10^7 [c]	2.93×10^7 (0.11)
α	0.259 (>5)[b]	0.219 (0.10)	1[c]
C(2)-H resonances			
δ_{C00}	3.81 (0.01)	3.82 (0.004)	3.82 (0.004)
δ_{C11}	4.89 (0.002)	4.89 (0.002)	4.90 (0.002)
ρ_C	0.756 (0.03)	0.740 (0.03)	0.733 (0.03)
δ_{D00}	3.75 (0.02)	3.75 (0.006)	3.75 (0.006)
δ_{D11}	4.85 (0.002)	4.86 (0.002)	4.86 (0.002)
ρ_D	0.756 (0.03)	0.740 (0.03)	0.733 (0.03)
C(4)-H resonances			
δ_{C00}	3.36 (0.009)	3.35 (0.009)	3.37 (0.008)
δ_{C11}	4.02 (0.002)	4.02 (0.002)	4.02 (0.002)
ρ_C	0.332 (0.22)	0.331 (0.18)	0.286 (0.21)
δ_{D00}	2.74 (0.02)	2.75 (0.01)	2.73 (0.01)
δ_{D11}	3.54 (0.002)	3.54 (0.002)	3.54 (0.002)
ρ_D	0.655 (0.05)	0.655 (0.05)	0.652 (0.04)
overall SD of the fit (ppm)	±0.014	±0.014	±0.013
$\bar{C}$[d]	0.54	0.47	0.76

[a] Values were obtained by fitting all the experimental pH titration data in Figure 4 simultaneously to models for mutual interaction between the two titrating imidazole groups given by eq 4 and 5. The standard deviations of the natural logarithms (SD_{ln}) of the optimized parameters are given in parentheses. For $SD_{ln} < 0.2$, $SD_{ln} \sim \Delta x/x$ where $\Delta x/x$ is the fractional error of the optimized parameter; for $SD_{ln} = 1$, the parameter value is determined to within a factor of $e \sim 2.72$; for $SD_{ln} >> 1$, the parameter is ill-determined. [b] These parameters, in addition to being ill-determined ($SD_{ln} > 5$), were highly correlated with correlation coefficients $r_{i,j}$ of $r_{K_{C0},K_{D0}} = r_{K_{C0},\alpha} = -1$ and $r_{K_{D0},\alpha} = 1$. [c] These parameters were not optimized and were constrained as follows: for model 1, $K_{C0} = K_{D0}$, and for model 2, $\alpha = 1$. [d] The mean absolute correlation index ($\bar{C}$) is a measure of the distribution of residuals [see Clore & Chance (1978) for the definition of $\bar{C}$]. For $\bar{C} \lesssim 1$, the distribution of residuals is random; for $\bar{C} >> 1$, there are systematic errors between the observed and calculated curves.

model 1: $K_{C0} = K_{D0}$; $\alpha \neq 1$ (7)

model 2: $K_{C0} \neq K_{D0}$; $\alpha = 1$ (8)

In both cases, all the chemical shift parameters (δ_{x00} and δ_{x11}) and dimensionless constants (ρ_x) were optimized; in addition, in the case of model 1, K_{C0} and α were optimized, and in the case of model 2, K_{C0} and K_{D0} were optimized. For both models, the overall standard deviations of the fits are within the overall standard error of the data (±0.015 ppm), the distribution of residuals is random, and the optimized parameters are well determined (see Table II). The comparison of the best-fit curves (which are indistinguishable for the two models) with the experimental data is shown in Figure 4, and the values of the optimized parameters together with their errors are given in Table II. Thus, we cannot distinguish whether the pKs of histidines C and D are initially identical with interaction occurring at both the thermodynamic and chemical shift levels (model 1) or whether the pKs of histidines

C and D are different with interaction only occurring at the chemical shift level (model 2). For model 1, we obtain $pK_{C0} = pK_{D0} = 7.16$ and $\alpha = 0.22$, and for model 2, $pK_{C0} = 6.21$, $pK_{D0} = 7.47$, and $\alpha = 1$. We also note that if the titration data for histidines C and D are fitted separately and no assumption is made as to the nature of the interacting group, then for both models the values of all the optimized parameters obtained are identical with those obtained when all the data are fitted simultaneously within the errors specified in Table II.

Discussion

Assignment of Histidines B and E. We have shown that histidines B and E reside in the small carboxy-terminal domain (see Figure 1). Examination of the amino acid sequence of CRP deduced from the nucletotide sequence of its structural gene shows that there are two histidine residues in the carboxy-terminal domain at positions 159 and 199 (Aiba et al., 1982; Cossart & Gicquel-Sanzey, 1982). Inspection of the crystal structure (McKay & Steitz, 1981) reveals that histidine-199, which is seven amino acid residues from the C-terminal end, probably lies in a region which is not well ordered in the electron density map and that histidine-159 is located either at the end of helix D or in the following loop structure. The ^{1}H NMR data show that histidine B is mobile on account of the narrow line widths of its imidazole proton resonances ($\sim$3 Hz), is readily accessible to the solvent with a $t_{1/2}$ for deuterium exchange of the C(2) proton of about 2 days, and has a pK value (7.07) and protonation shift values [0.99 and 0.47 ppm for the C(2) and C(4) proton resonances, respectively] within the ranges of those found for histidine residues in small peptides (Markley, 1975). In contrast, the line width of the C(2) proton resonance of histidine E is broad ($\sim$15 Hz), its C(2) proton is essentially inaccessible to the solvent, no significant deuterium exchange being noted after 50 days at 37 °C, and its pK is abnormally low ($\lesssim$5) for a histidine residue, suggesting that it lies buried and partially immobilized within a rigid portion of the protein in the deprotonated state at physiological pH values. Moreover, it seems likely that histidine E lies in the vicinity of a group with a high pK (which is therefore protonated at physiological pH values) as interaction of a histidine residue with a positively charged group would lower the pK of that histidine residue, thus accounting for the low pK of histidine E. In this respect, we note that the carboxy-terminal domain contains a large number of basic amino acid residues (Aiba & Krakow, 1981; Aiba et al., 1982; Cossart & Gicqel-Sanzey, 1982) which could function in this manner. Although we cannot assign with certainty which of the two histidine resonances in the sequence of the carboxy-terminal domain corresponds to histidines B and E, we tentatively assign histidine B to histidine-199 and histidine E to histidine-159 on the assumption that it is more likely for the histidine residue very close to the C-terminal end, namely, histidine-199, to be the more mobile amino acid.

Assignments of Histidines A, C, and D. Histidines A, C, and D reside in the N-terminal domain of CRP. Amino acid analyses of CRP, αCRP, and a number of other CRP fragments have all shown that there are a total of five histidine residues in CRP, three of which reside in the N-terminal domain (Anderson et al., 1971; Aiba & Krakow, 1981), in complete agreement with our ^{1}H NMR data. In contrast, the amino acid sequence of CRP deduced from the nucleotide sequence of its structural gene contains six histidine residues, four of which are in the N-terminal domain (Aiba et al., 1982; Cossart & Gicquel-Sanzey, 1982). The latter are at positions 17, 19, 21, and 31. Examination of the X-ray width structure (McKay & Steitz, 1981) shows that histidines-17, -19, and -21 probably lie in the first β-pleated sheet and that histidine-31 lies in either the second or third β-pleated sheet. The ^{1}H NMR data show that histidines A, C, and D are all freely accessible to the solvent with a $t_{1/2}$ of about 2 days for deuterium exchange of their C(2) protons (Figure 2). The imidazole ring of histidine A shows classical Henderson–Hasselbach behavior, titrating with a single pK of 6.68 and protonation shifts of 0.98 and 0.45 ppm for the C(2) and C(4) proton resonances, respectively. In contrast, histidines C and D titrate with their imidazole rings mutually interacting (see Figure 4 and Table II). One of the common features of β-pleated sheets in proteins is the fact that the side chains of neighboring amino acid residues lie on opposite sides of the α-carbon backbone. Thus, the imidazole rings of histidines-17, -19, and -21 lie on the same side of the β-pleated sheet. Model building shows that for two histidine residues separated by a single amino acid residue on a β-pleated sheet, the separation between the two imidazoles will lie within the range 2–8 Å. This is close enough to allow the two imidazole rings to interact, for example, by hydrogen bonding, and to compete for the same proton. The minimum distance between the imidazole rings of two histidine residues separated by three other residues on a β-pleated sheet, however, is greater than 10 Å, which is probably too large to allow for any significant interaction between them. We therefore suggest tentatively that histidine A corresponds to histidine-31 and that histidines C and D correspond either to histidines-17 and -19 or to histidines-19 and -21.

At present, we are unable to resolve the discrepancy in the number of histidine residues in CRP obtained from amino acid analysis on the one hand (Anderson et al., 1971; Aiba & Krakow, 1981) and from the nucleotide sequence on the other (Aiba et al., 1982; Cossart & Gicquel-Sanzey, 1982). Suffice it to say that the ^{1}H NMR data are consistent with the amino acid analysis, and we are unable to see a set of titratable resonances which could correspond to a sixth histidine residue. If indeed there is a sixth histidine residue in CRP, it must have very unusual properties.

Acknowledgments

We thank Sir Arnold Burgen for continual encouragement and support. We also thank Dr. B. Blazy and Professor A. Baudras for stimulating and helpful discussions and for their generous gift of CRP and αCRP.

References

Aiba, H., & Krakow, J. S. (1981) *Biochemistry 20*, 4774–4780.

Aiba, H., Fujimoto, S., & Ozaki, N. (1982) *Nucleic Acids Res. 10*, 1345–1362.

Anderson, W. B., Schneider, A. B., Emmer, M., Perlman, R. L., & Pastan, I. (1971) *J. Biol. Chem. 246*, 5929–5973.

Clore, G. M., & Chance, E. M. (1978) *Biochem. J. 175*, 709–725.

Cossart, P., & Gicquel-Sanzey, B. (1982) *Nucleic Acids Res. 10*, 1363–1378.

Edsall, J. T., Martin, R. B., & Hollingworth, R. B. (1958) *Proc. Natl. Acad. Sci. U.S.A. 44*, 505.

Eilen, E., Pampeno, C., & Krakow, J. S. (1978) *Biochemistry 17*, 2469–2473.

Gronenborn, A. M., & Clore, G. M. (1982) *Biochemistry* (preceding paper in this issue).

Krakow, J. S., & Pastan, I. (1973) *Proc. Natl. Acad. Sci. U.S.A. 70*, 2529–2533.

Markley, J. L. (1975) *Acc. Chem. Res. 8*, 70–80.

McKay, D. B., & Steitz, T. A. (1981) *Nature (London) 290*, 745–749.
Powell, M. J. D. (1972) Atomic Energy Research Establishment Report No. TP.492, Harwell, England.
Riggs, A. D., Reiness, G., & Zubay, G. (1971) *Proc. Natl. Acad. Sci. U.S.A. 68*, 1222–1225.
Schrager, R. I., Cohen, J. S., Heller, S. R., Sachs, D. H., & Schecter, A. N. (1972) *Biochemistry 11*, 541–547.
Takahashi, M., Blazy, B., & Baudras, A. (1980) *Biochemistry 19*, 5124–5130.
Takahashi, M., Gronenborn, A. M., Clore, G. M., Blazy, B., & Baudras, A. (1981) *FEBS Lett. 139*, 37–40.

Cholesterol Desorption from Clusters of Phosphatidylcholine and Cholesterol in Unilamellar Vesicle Bilayers during Lipid Transfer or Exchange†

Larry R. McLean‡ and Michael C. Phillips*

ABSTRACT: The rate of [4-^{14}C]cholesterol transfer from phosphatidylcholine (PC) small unilamellar vesicles of different acyl chain compositions and cholesterol concentrations has been followed as a function of temperature in the presence of excess acceptor vesicles. Cholesterol–PC vesicles containing either egg PC, dimyristoyl-PC (DMPC), or dipalmitoyl-PC (DPPC) were used as either donor or acceptor vesicles. One population of vesicles contained 15 mol % dicetyl phosphate to confer a negative charge so that the donor and acceptor vesicles could be separated rapidly by ion-exchange chromatography. The rate of cholesterol transfer from negatively charged 20 mol % cholesterol–egg yolk PC vesicles to pure egg PC, DMPC, or DPPC vesicles was followed over a temperature range which included the gel to liquid-crystal transition temperatures (T_c) of the saturated PC acceptor vesicles. The Arrhenius plots for all three systems are linear and superimposable so that the activation energy (E_a) is close to 88 kJ/mol in every case. Thus, neither the rate nor the E_a for transfer is dependent upon the physical state of the hydrocarbon chains in the acceptor vesicles when acceptor vesicles are in excess; this is consistent with earlier findings that under such conditions the rate of cholesterol transfer is determined by the rate of cholesterol desorption from the donor vesicle bilayer into the aqueous phase. The rate of cholesterol desorption from donor vesicles containing 1 mol % cholesterol in either egg PC, DMPC, or DPPC bilayers was followed at temperatures above and below the T_c of the donor vesicles. The rate constant for cholesterol desorption from egg PC bilayers is greater by an order of magnitude than for DMPC or DPPC bilayers. For all three host lipids, the Arrhenius plots do not show any significant deviations from linearity, and the E_a values above and below the T_c of the DMPC or DPPC vesicles do not differ significantly. Thus, the rate of cholesterol desorption is not influenced by the physical state of the phospholipids which can undergo chain melting in the donor bilayer but is strongly dependent on nearest-neighbor interactions. The first-order rate constant for cholesterol desorption from egg PC bilayers containing 5–40 mol % cholesterol is essentially constant ranging from 0.81×10^{-4} s^{-1} to 1.33×10^{-4} s^{-1}. These data suggest that cholesterol desorbs from a region of the bilayer which is laterally phase separated from the free-melting phospholipid. The cholesterol flux data are analyzed in terms of a model in which cholesterol desorption occurs from equimolar cholesterol–PC clusters in the bilayer. The rate of cholesterol desorption from PC bilayers containing 1–40 mol % cholesterol is proportional to the fraction of bilayer covered by equimolar PC–cholesterol clusters and is sensitive to the cholesterol–PC hydrocarbon chain interactions in such clusters.

An important aspect of cellular lipid metabolism is the exchange and transfer of cholesterol between cell membranes and lipoproteins [for a review, see Smith & Scow (1979)]. In a previous report (Phillips et al., 1980) we have shown that transfer of cholesterol from cells in culture to acceptors in the medium proceeds by diffusion of cholesterol through the aqueous phase. In order to investigate lipid exchange under carefully controlled conditions, we have also followed cholesterol and phosphatidylcholine (PC)[1] exchange between unilamellar vesicles (McLean & Phillips, 1981). In this system aqueous diffusion is also operative for exchange of both bilayer lipids. This conclusion for cholesterol exchange between unilamellar vesicles has been confirmed by Backer & Dawidowicz (1981). Aqueous diffusion proceeds as a two-step process: (1) desorption of cholesterol from a donor bilayer membrane into the aqueous phase and (2) adsorption of cholesterol from the aqueous phase into an acceptor bilayer. When acceptor vesicles are in excess, desorption is the rate-limiting step for exchange, and the rate of cholesterol exchange is independent of the concentration of the acceptor vesicles in the incubation mixture (McLean & Phillips, 1981).

A number of workers (Bloj & Zilversmit, 1977; Poznansky & Lange, 1978; Nakagawa et al., 1979) have shown that the rate of cholesterol exchange from sonicated cholesterol–PC donor vesicles of different acyl chain composition to various acceptors depends on the acyl chain composition of the donor vesicle bilayer PC. These data suggest that the physical state

† From the Department of Physiology and Biochemistry, The Medical College of Pennsylvania, Philadelphia, Pennsylvania 19129. *Received January 7, 1982.* This research was supported by Program Project Grant HL 22633 and Institutional Training Grant HL 07443 from the National Heart, Lung and Blood Institute. A portion of this work was accepted by the faculty of the Medical College of Pennsylvania in partial fulfillment of the degree of Doctor of Philosophy awarded to L.R.M.

‡ Present address: Biochemistry Department, the Royal Free Hospital School of Medicine, University of London, London WC1N 1BP, England.

[1] Abbreviations: DEAE, diethylaminoethyl; PC, phosphatidylcholine; DMPC, dimyristoylphosphatidylcholine; DPPC, dipalmitoylphosphatidylcholine; SEM, standard error of the mean; PNA, 9-(3-pyrenyl)nonanoic acid; DSC, differential scanning calorimetry.

0006-2960/82/0421-4053$01.25/0